2015 ASIA-PACIFIC SOLAR RESEARCH CONFERENCE

Peer Reviewed
2015 Solar Research Conference

Kanyawee Keeratimahat

Temperature Estimation of an Unconventional PV Array using the Sandia Module Temperature Model

K. Keeratimahat[1], A. G. Bruce[1], J. K. Copper[1] and R. Evans[1]
[1]*School of Photovoltaic and Renewable Energy Engineering, University of New South Wales, Sydney, Australia*
E-mail: k.keeratimahat@student.unsw.edu.au

Abstract

Several models to predict PV module or cell temperature as a function of the weather have been developed. This study focuses on the module temperature model proposed by Sandia National Laboratory (SNL) as this model is one of the models available for use within NREL's System Advisor Model (SAM). Although many studies have found that the SNL model can predict module temperatures with relatively small errors, the majority of these studies analysed PV modules on conventional mounting structures. As the cost of PV modules decreases, optimising tilt and orientation to maximise energy production is less critical to the economics of PV projects, while there is increasing interest in array layouts that prioritise other aspects of array design, such as low cost mounting structures and energy production that coincides with peak electricity load. It is therefore important to assess the feasibility of using existing module/cell temperature models, like the SNL model in SAM, to model unconventional array mounting structures.

This paper analyses the applicability of the SNL model for an unconventional mounting configuration by solving the empirical parameters of the SNL model to experimental measurements of module temperature and wind speed. The analysis is performed for an open-circuited east-west facing array with the array mounted directly on the ground. This mounting configuration was expected to result in reduced air flow behind the module in comparison to a standard rack-mounting configuration, resulting in a different temperature response of the modules for the same weather conditions. It was found that for this mounting structure, wind speed influences the slope of the linear relationship between module temperature and irradiance. The empirical parameters of the SNL model are established; however these should be interpreted as preliminary values, given the limited time period and weather conditions under which the study was undertaken. The model tends to underestimate module temperature at higher ambient temperature, which implies that underestimation would occur in summer if these parameters are used. Nonetheless, the results indicate that the temperature pattern of the unconventional array can be predicted with an acceptable error using SNL's temperature model.

1. Introduction

When designing a mounting structure, it is important to understand how it will perform in the field so that its effect on the energy output of a PV array can be estimated. Module/cell operating temperature is one of the most important factors affecting PV performance, as it can significantly reduce the energy output of a PV system, and should therefore be accounted for when modelling PV performance with novel mounting structures. The simplest methods

typically employed to account for temperature effects on PV performance use manufacturer temperature coefficients for power, voltage and current, or nominal operating cell temperature (NOCT). The temperature coefficients are calculated under standard test conditions (irradiance = 1000 W/m^2, air temperature = 25°C), whilst NOCT is defined as the mean cell temperature for an open rack mounted module under the standard reference environment (irradiance = 800 W/m^2, air temperature = 20°C, wind speed = 1 m/s) as defined in IEC61215 (2005). Although both of these methods can provide a guide to the temperature at which a module will operate within the field, the actual operating temperature at any particular time depends on the local climate conditions such as wind speed, irradiance and ambient temperature at that point in time. Moreover, the type of mounting structure and module material also has an influence. In addition, Muller (2010) points out that NOCT does not take into account the effect of heat transfer parameters of sky and ground temperature and does not explain temperature variation relating to climate or atypical mounting configurations. A more comprehensive model, that is a function of meteorological factors and the mounting configuration, should ideally be used to improve the estimation of module temperature.

Several models to predict PV module or cell temperature as a function of the weather, module material and the mounting configuration have been developed. One such model is the Sandia National Laboratory (SNL) module temperature model which defines module temperature as a function of plane of array irradiance (POA), ambient temperature, wind speed and two model coefficients (*a* and *b*) which are dependent on the module construction and materials as well as the mounting configuration of the module (King et al., 2004). The pre-defined parameters of the SNL model are limited to two conventional mounting structures: open-rack and close roof mount (or insulated back); and two module materials/construction types: glass/cell/glass and glass/cell/polymer sheet. These pre-defined parameters may not be suitable to predict module temperatures of atypical mounting configurations

The objectives of this study are to evaluate and analyse the temperature performance of a atypical mounting structure, with a particular focus on how module temperatures are affected by irradiance and wind speed. To undertake this assessment, measured module temperatures from an experimental setup are compared to estimates of module temperatures using the NOCT and Sandia Nation Laboratory (SNL) module temperature models. As part of this study, the empirical parameters of the module temperature model proposed by Sandia National Laboratory (SNL) (*a* and *b*), will be calculated for the atypical mounting configuration assessed in this study. Further, the differences between the modelled and measured module temperatures will be discussed.

The experimental array is an east-west facing array mounted near-ground level (Figure 1), where the gap at each ridge of the array is small and suspected to result in less ventilation compared to the conventional rack mounting structure. The array is open circuited in order to eliminate the problem of non-uniform temperature distribution due to the non-homogeneities within the modules, as no power is being dissipated at open circuit. The SNL module temperature model is one of the available module/cell temperature models available for use within NREL's System Advisor Model (SAM), an open source renewable energy system modelling tool, which has an option for user defined values of the SNL model coefficients, *a* and *b*.

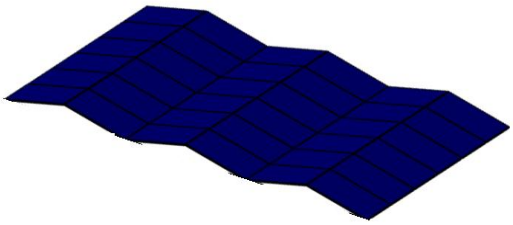

Figure 1. A model of the new mounting structure array

Figure 2. The site

2. Methodology

2.1. Description of unconventional array

The array is located at 33.98°S, 150.99°E in south Sydney, and consists of 24 modules, with 8 rows and 3 modules per row (Figure 2). The modules used in the array are 300W polycrystalline silicon from Jinko (JKM300P-A) with glass cover and back polymer sheet. All modules are left open-circuited for the purposes of this experiment. The location is a relatively unused industrial site, and is surrounded by ridges on the east and south. The prototype was constructed such that there is no nearby shading at any time of the day.

2.2. Monitoring system

The monitoring system utilises an Arduino Uno data logger (Fuentes et al., 2014). This device is a terminal hub for all measurement sensors including the module temperature sensors and the pyranometer. The pyranometer measures global horizontal irradiance which is then translated to POA irradiance utilising the Perez irradiance transposition model (Copper et al., 2013). The data is collected every 10 minutes over 3G connections. Five temperature probes are attached to the centre back of west facing modules at different positions shown in Figure 3. This experiment uses DS18B20 digital temperature sensors and a first class amplified pyranometer Middleton Solar SK08-E. The ambient temperature sensor is the same model as the ones attached to the modules and it is placed in a radiation shield to prevent the influence of heat from radiation and the cooling effect of wind. The mounting of the ambient temperature sensor is installed 1 m above the ground.

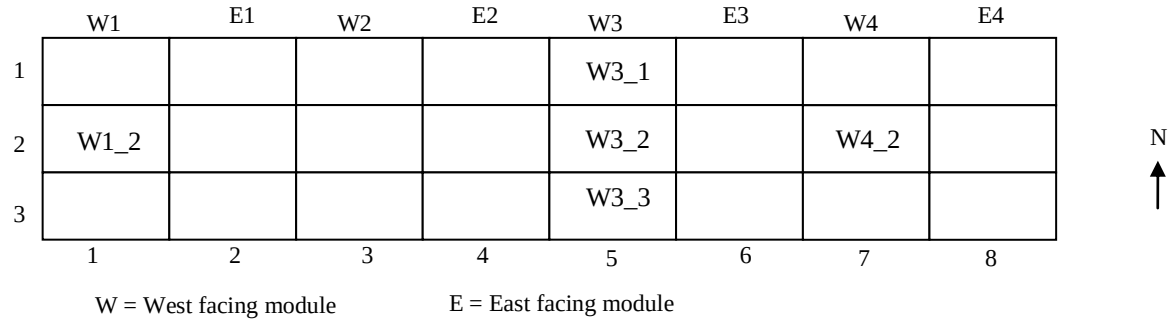

Figure 3. The layout of temperature sensor positions

2.3. Data Collection

The monitoring system was set up in July 2015 and the data analysed in this experiment was collected over 2 months from August to September 2015. Due to the absence of on-site wind speed measurement, the wind speed data used for this experiment is obtained from a nearby BOM weather station at Holsworthy airport (Station ID: 066161) which is located 4 km away from the site. Wind speed is being scaled from the weather to the site by Eq 1 (Burton et al., 2011),

$$u(z) = u(z_{ref}) \frac{\ln(\frac{z}{z_0})}{\ln(\frac{z_{ref}}{z_0})}, \quad \text{Eq 1}$$

where z is the interested height (m), z_{ref} is the reference height at the original location that data is measured (m), z_0 is the surface roughness (m) and $u(x)$ is the wind speed according to the height at x metres.

Within the data set, there are periods of missing data from intervals of 10 minutes up to several weeks. The short term missing data (less than 2 hours) was usually due to a miss-sent signals and this data was estimated using linear interpolation. The data missing for longer terms was due to data logger breakdown for up to 2 to 3 weeks before the device was fixed. Data from these time periods were omitted

3. Data Evaluation

The frequency histogram of averaged measured module temperatures across the array (Figure 4), when the POA irradiance is more than 200 W/m^2, shows that most of average temperatures (52%) fall within the range of 35^{o}C to 50^{o}C, with a maximum of 54^{o}C and a minimum of 13.2^{o}C recorded. The data corresponding to irradiance below 200 W/m^2 were excluded to exclude night time temperatures and the period of sunrise and sunset where the modules start to gain and lose heat. Figure 5 shows the same data plotted as the difference between the module temperature and the ambient temperature. The maximum difference between the average array temperature and the ambient temperature is 30.3^{o}C but difference lies between 25^{o}C to 30.3^{o}C for most of the time (Figure 5).

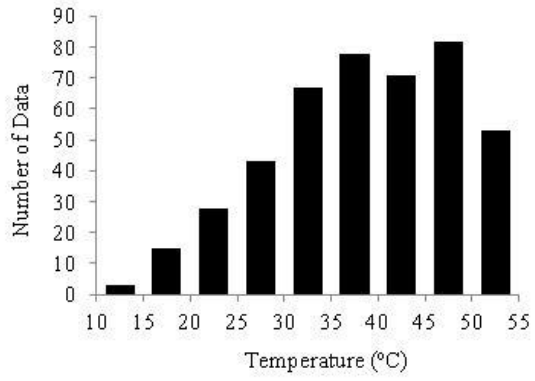

Figure 4. Frequency histogram of the average temperatures of all 5 modules for POA irradiance > 200 W/m^2

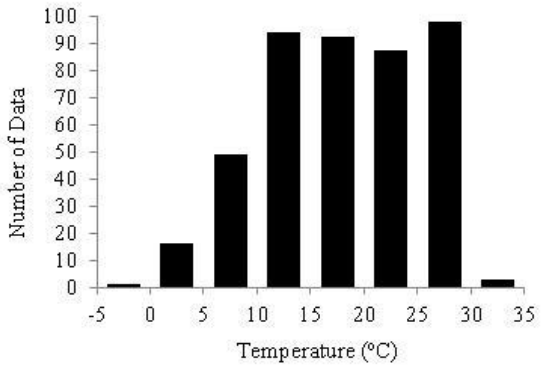

Figure 5. Frequency histogram of the difference between the average module temperature and the ambient temperature when POA irradiance > 200 W/m^2

The increase in module temperature above the ambient can also be plotted as a function of irradiance, and categorised according to wind speed bins, as shown in **Figure 6**. This method

is used by Koehl et al. (2011) to show the dependence of module temperature on irradiance and wind speed. The same set of data as used in Figure 4 and 5 (i.e. above 200 W/m^2) is also used for this analysis to avoid high variability in the morning and evening times due to low solar altitude angles which could skew the results. Figure 6 also plots the linear lines of best fit for each of the wind speed bins, indicating that the slopes of the lines of best fit are different for each wind speed bin. At high wind speed (5 to 7 m/s), it can be seen that the linear relationship between the POA irradiance and the difference in temperature deteriorates, as evidenced by the decreasing R-value shown in Table 1. At the wind speed of 6 to 7 m/s, the difference in temperatures can no longer be explained by the irradiance as a linear function (R-squared = 0). This may be caused by the heat transfer due to forced convection. At low wind speeds, it can be assumed that irradiance is the dominant element influencing the temperature differential, assisted by natural convection. The results for high wind speeds could also be an issue with data quality, particularly as the wind sensor is remote from the site.

This data fits the form of SNL's temperature model (Eq 2) (Koehl et al., 2011) where the exponential term in the equation can be assigned as a slope x of a linear function $T_m = T_a + xG$ where x is $e^{(a+b\cdot v_w)}$. The two parameters, a and b (typically negative values) are fixed and are dependent on the type of mounting configuration and module material/construction, hence the only variable in this equation is the wind speed,

$$T_m = T_a + G[e^{(a+b\cdot v_w)}] \qquad \text{Eq 2}$$

where T_m is back module temperature , T_a is ambient temperature, G is POA irradiance [W/m^2], a is a dimensionless coefficient describing the effect of the radiation on module temperature, b is the cooling by the wind [s/m] and v_w is wind speed [m/s].

The expected characteristic of the lines of best fit dictate that lower wind speeds should result in steeper slopes. The increase in wind speed, in terms of the exponential function, will result in a lower value for the coefficient x. In this analysis, the individual slopes do not always perfectly follow the expected trend; however the overall plot of slope versus wind speed (Figure 7) indicates a general linear trend in which the slope decreases with increasing wind speeds.

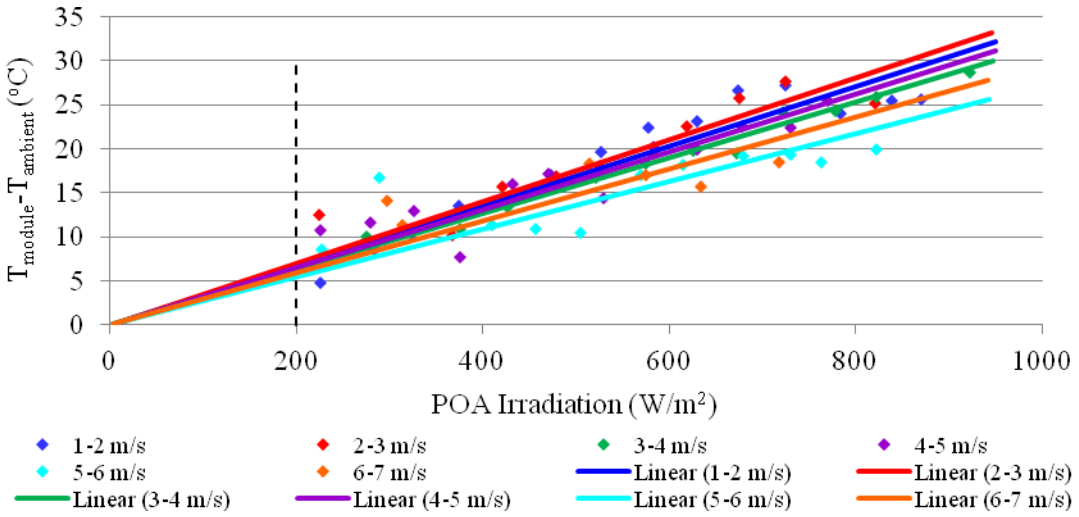

Figure 6. Difference between the average module temperatures and the ambient temperature as a function of POA irradiance categorised by wind speed bin. The data is the average of the difference in temperature within an irradiance bin of 50 W/m^2.

Additionally, testing the null hypothesis that there is no correlation between the slopes and the wind speeds results in a p-value of 0.049 which is less than 0.05. This is an enough evidence to reject the null hypothesis and conclude the slope is related to wind speed in the way it is expected to. These relationships may be weak due to the use of remote wind data, which may not reflect conditions on site due to the local terrain and/or due to the small sample size of the dataset. Nonetheless, the correlation between wind speed and slope does demonstrate that remote measurements of wind speed are useful in the absence of onsite measurements.

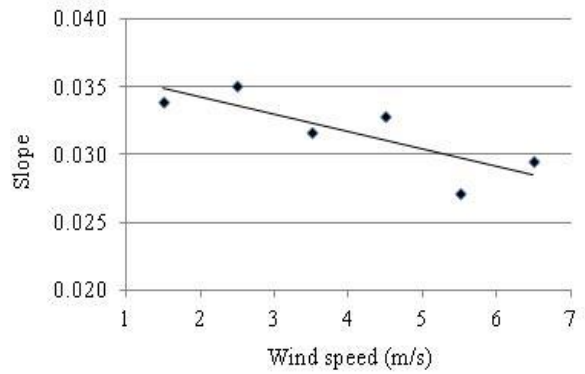

Figure 7. Plot of slope vs. wind speed

Table 1. Slope and R-squared value of the lines in Figure 6.

Wind Speed (m/s)	Slope	R-square
1-2	0.0339	0.890
2-3	0.0351	0.881
3-4	0.0316	0.983
4-5	0.0328	0.805
5-6	0.0272	0.372
6-7	0.0295	0

4. Temperature modelling

4.1. NOCT Model

IEC61215 (2005) defines NOCT as the cell temperature in a 45° tilted, open rack mounted module exposed to 800 W/m^2 irradiance at 20°C ambient temperature with wind speed of 1 m/s. The module temperature can be modelled by Eq. 3 where the NOCT provided by the manufacturer of the module used in this study is 45°C. The result of the prediction shows that NOCT tends to underestimate module temperatures at high levels of irradiance (Figure 8). A comparison between NOCT and Sandia models will be discussed further in Section 5.

$$T_m = T_{amb} + (NOCT - 20)\left(\frac{E}{800}\right) \quad \text{Eq 3}$$

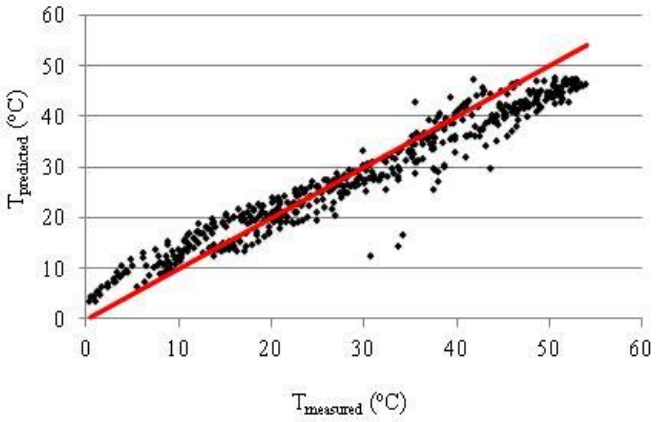

Figure 8. Plot of predicted temperature by NOCT and measured temperature

4.2. SNL Model

4.2.1. Normalised mean bias error (NMBE) method

Using the data when POA is not zero, the coefficients of the SNL module temperature model (*a* and *b* in Eq 2) were determined via the solver function available within MS Excel. The solver function was implemented by solving the normalised mean bias error (NMBE) equal to zero. The values of *a* and *b* utilised to initiate the solver function were based on the coefficients of a linear line of best fit of the measured data. The results of the analysis are shown in Table 2, where the average parameters are derived from the average temperature data of all modules.

The results indicate that the wind speed factor, *b*, varies significantly across the different module positions within the array as evidenced by the normalised standard deviation. The pre-existing SNL values of *a* and *b* used in this analysis were for the glass/cell/polymer sheet and open rack mounting configuration. This set of pre-defined values achieved the highest correlation to the measured temperature, amongst the available list of pre-defined values. In comparison to the results using the pre-defined set of SNL model coefficients, the solved coefficients show a significant improvement in the modelled module temperatures as indicated by the significantly lower levels of RMSE reported in Table 2.

Table 2. The parameters for SNL's temperature model and the errors associated with them by solving NMBE

Module	a	b [s/m]	MBE [^{o}C]	NMBE	MAE [^{o}C]	MAPE	RMSE [^{o}C]	NRMSE	Pearson Coefficient
SAM Value	-3.56	-0.075	-3.63	-12.25%	4.85	21.35%	6.01	20.30%	0.55
W1_2	-3.38	-0.011	0.00	0.00%	3.07	20.94%	3.96	13.45%	0.96
W3_1	-3.47	0.033	0.00	0.00%	2.98	15.68%	3.93	13.13%	0.96
W3_2	-3.39	0.008	0.00	0.00%	3.20	21.35%	4.11	13.66%	0.96
W3_3	-3.45	0.003	0.00	0.00%	3.00	21.93%	3.84	13.18%	0.96
W4_2	-3.44	0.002	0.00	0.00%	2.93	18.75%	3.74	12.79%	0.96
Average	-3.43	0.01	-0.03	-0.09%	2.99	18.12%	3.86	13.04%	0.96
Std dev.	0.04	0.02							
Std dev %	1.17	226.66							

4.2.2. Mean absolute error (MAE) method

A similar analysis was undertaken by solving to minimise the MAE. MAE only considers the magnitude of the residuals, which therefore impacts how errors are treated for measurements approaching zero. This method gives less variation in the solved wind speed factors with minimal impact on the overall accuracy of the modelled results (Table 3).

Figure 9 clearly shows that the dispersion of the residuals via this method is less than observed for the method solving for NMBE. The prediction by NMBE results in minimal bias while the overall uncertainty (NRMSE) is lower via the MAE method. However, in this case, MAE can predict the temperature at high irradiance more accurately and the overall uncertainty is reduced as 23.73% of the predicted temperatures fall within the error range of -1 to 1 ^{o}C, compared to the NMBE method, which only resulted in 17.12% of predicted values falling within this range. Hence, the parameters obtained from the analysis using MAE, *a* is -3.20 and *b* is -0.074, will be used for the temperature model of this non-standard mounting.

Table 3. The parameters for SNL's temperature model and the errors associated with them by solving MAE

Module	a	b [s/m]	MBE [°C]	NMBE	MAE [°C]	MAPE	RMSE [°C]	NRMSE	Pearson Coefficient
SAM Value	-3.56	-0.075	-3.63	-12.25%	4.85	21.35%	6.01	20.30%	0.55
W1_2	-3.15	-0.076	0.55	1.86%	2.93	21.43%	3.93	13.34%	0.96
W3_1	-3.15	-0.068	0.39	1.31%	2.65	15.66%	3.64	12.16%	0.96
W3_2	-3.12	-0.068	0.54	1.80%	3.01	21.84%	4.00	13.29%	0.96
W3_3	-3.44	-0.024	-0.73	-2.50%	2.98	21.59%	3.89	13.35%	0.97
W4_2	-3.13	-0.090	0.58	1.98%	2.68	19.06%	3.58	12.24%	0.97
Average	**-3.20**	**-0.07**	**0.53**	**1.78%**	**2.77**	**18.50%**	**3.72**	**12.58%**	**0.96**
Std dev.	0.14	0.02							
Std dev %	4.23	37.65							

5. Comparison between NOCT and SNL's temperature model

Table 4 demonstrates that the mean absolute error associated with the SNL module temperature model is reduced by 35% compared to the prediction using the NOCT model (Eq 3). Additionally, the improvement in predicting from NOCT to SNL's model at higher module temperatures can be seen by comparing Figure 11 to Figure 8. However, the prediction from the NOCT model is still reasonable. The majority of the differences between the modelled and measured values by the NOCT model lie within ±1°C. This is similar to the results of the SNL model (Figure 10) even though the prediction was expected to be worse. The reason could be that most of the experimental data was collected under climate conditions similar to the requirements of NOCT (i.e. irradiance = 800 W/m^2, air temperature = 20°C) since the period of data collection was during winter. Hence the site had not experienced any extreme climate condition such as ambient temperatures greater than 30^{o}C and irradiance greater than 920 W/m^2. In this situation, using NOCT for module temperature prediction is expected to work reasonable well. Likewise, the applicability of the SNL model coefficients presented in this paper may also only hold true for this winter set of climate conditions. Figure 12 demonstrates that the SNL model tends to underestimate module temperatures at higher ambient temperature. The dataset used in this figure was filtered for irradiance above 400 W/m^2 to illustrate the response of the model at high ambient temperatures and irradiance levels which would be expected during summer.

Table 4. Comparison between errors of NOCT and SNL temperature models

Model	MBE [°C]	NMBE	MAE [°C]	MAPE	RMSE [°C]	NRMSE	Pearson Coefficient
Sandia	0.53	1.78%	2.77	18.50%	3.72	12.58%	0.96
NOCT	-1.21	-4.10%	4.84	28.56%	4.18	14.17%	0.97

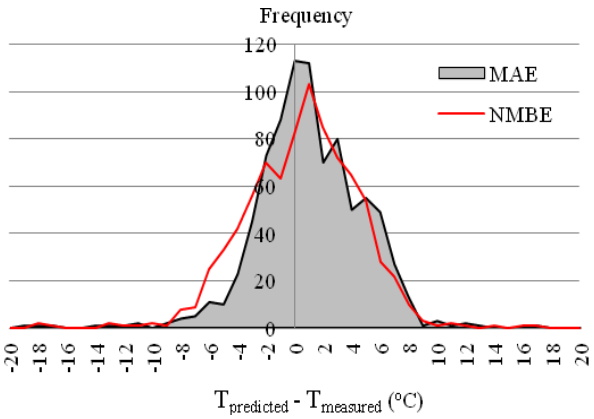

Figure 9. Frequency distributions of errors in prediction of SNL's model by MAE and NMBE methods relative to measured temperatures

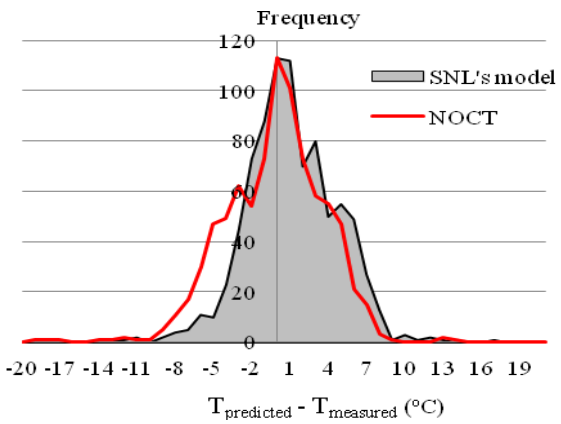

Figure 10. Frequency distributions of the difference betweem predicted and measured modules temperature of SNL's temperature model and NOCT

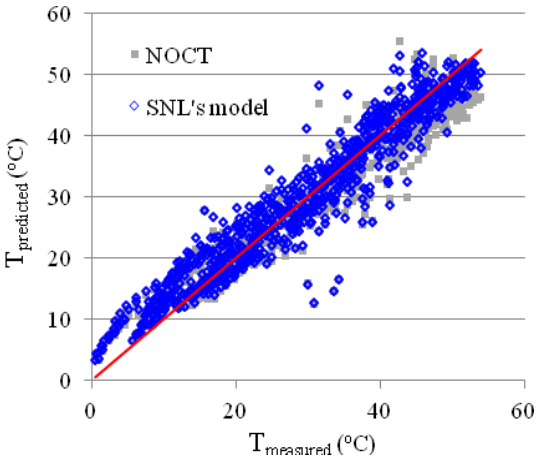

Figure 11. Plot of predicted against measured module temperatures between NOCT and SNL's temperature model.

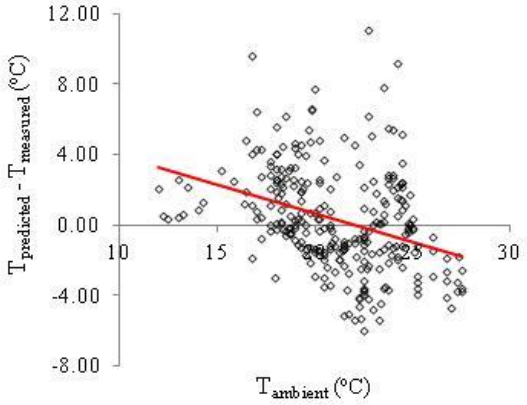

Figure 12. Scatter plot of the difference between predicted and meausred moduel temperature of SNL's temperature model as a function of ambient temperature. (A red line is added to show the trend.)

6. Conclusions

This study has investigated the dependence of module temperatures on POA irradiance, ambient temperature and wind speed by using statistical approaches. The data evaluation has shown that the wind speed data from a nearby off-site weather station can be validly applied to the site, although an onsite wind speed measurement sensor would improve the accuracy of the results, because the wind speed at this site cannot be simply scaled from the remote wind data due to the characteristic of the terrain. Nevertheless, a strong correlation between the effects of remote wind data on the module temperatures is presented.

The parameters *a* and *b* for the new mounting structure studied in this experiment are found to be -3.20 and -0.074, respectively. This implies that the temperature of this prototype can be modelled by SNL's module temperature model. However, underestimation of module temperatures are likely to occur if the parameters found in this analysis are used to predict module temperatures in summer when the ambient temperature could be more than 40^{o}C at

the site. It can be concluded that the SNL module temperature model has a potential in predicting the temperature of this new mounting structure but the parameters derived in this experiment may not be applicable to predict the module temperatures of this prototype during a summer period. It is therefore recommended that the data should be collected for a longer period of time and over various seasons in order to derive representative parameters in the temperature model for this new mounting structure.

The analysis highlights the importance of a reliable monitoring system for this type of study, as inconsistent data logging such as inconsistent timestamp or missing data introduce uncertainties to the results. Although this study used linear interpolation to fill missing data, this method may miss temperature changes due to abrupt cloud transients or wind gust.

References

Bureau of Meteorology 2015. 'Latest Weather Observations for Holsworthy'. *In:* Australian Government Bureau of Meteorology.

Burton, T., Jenkins, N., Sharpe, D. & Bossanyi, E. 2011. The Wind Resource. *Wind Energy Handbook.* John Wiley & Sons, Ltd.

Copper, J., Bruc, A., Spooner, T., Martina, Calais, Pryor, T. & Watt, M. 2013. 'Australian Technical Guidelines for Monitoring and Analysing Photovoltaic Systems Version 1.'. Australian PV Institute.

Fuentes, M., Vivar, M., Burgos, J. M., Aguilera, J. & Vacas, J. A. 2014. Design of an accurate, low-cost autonomous data logger for PV system monitoring using Arduino™ that complies with IEC standards. *Solar Energy Materials and Solar Cells,* 130**,** 529-543.

International Electrotechnical Commission 2005. 'IEC 61215 Ed. 2.0 (English 2005)'. *Crystalline silicon terrestrial photovoltaic (PV) modules - Design qualification and type approval.*

King, D. L., Boyson, W. E. & Kratochvill, J. A. 2004. 'Photovoltaic Array Performance Model'. *Sandia Report.* Sandia National Laboratories.

Koehl, M., Heck, M., Wiesmeier, S. & Wirth, J. 2011. Modeling of the nominal operating cell temperature based on outdoor weathering. *Solar Energy Materials and Solar Cells,* 95**,** 1638-1646.

Muller, M. 2010. 'Measuring and Modeling Nominal Operating Cell Temperature (NOCT)'. NREL.

Acknowledgements

The experiment was partially funded by School of Photovoltaic and Renewable Energy Engineering, University of New South Wales.

We thank our colleagues for field experimental setup and data logger programming. Lastly, we would also like to show our gratitude to 5B Australia for creating the prototype and allowing us to conduct the study.